# *Inferences of a Layered Structure from S Wave Spectra Part 3. SH and SV Waves and Some Related Problems*

By
Takeshi MIKUMO
*Disaster Prevention Research Institute, Kyoto University*
and
Tuneto KURITA*
*Department of Transportation Engineering, Faculty of Engineering, Kyoto University*

**Abstract**

An attempt is made to infer the crust-mantle structure in several regions of Japan and North America from the spectral amplitude ratio and the phase difference between SH and SV waves from deep shocks.

It is found that the spectral behaviors of well-recorded S waves give support to some of the probable structures derived from P wave spectrum and some other information, suggesting characteristic differences in the tectonic structures; the possible existence of a rather thick intermediate layer having velocities between those appropriate to the lower crust and the normal mantle over three regions of Japan; and of a typical continental structure and oceanic crust in selected two regions of North America.

The structures inferred for central and eastern Japan can explain satisfactorily the observed phase velocities of Rayleigh waves, but the Love wave velocities are significantly higher than those expected from the structures. If the high velocities of Love waves are not a result of higher mode contamination, the observed inconsistency may be accounted for either by anisotropic (transversely isotropic) mantle or laminated mantle models, but the spectral behaviors of S waves appear to favor the former model.

## §1. Introduction

It has been shown in several recent investigations that the spectrum of seismic body waves can be effectively used to infer the underground structure immediately beneath a recording station, since PHINNEY (1964) first presented a method of using the spectral amplitude ratio on the basis of the Thomson-Haskell matrix method (HASKELL, 1962). KURITA (1969a, b; 1970) has successfully determined the crustal and upper mantle structure in three selected regions of Japan from both the amplitude and phase spectra of long-period P waves from a number of distant earthquakes.

In Part 1 of this paper (KURITA and MIKUMO, 1971), we presented the corresponding method for the case of S waves by testing their spectral response to various layered models. In Part 2, KURITA (1971) gave some results of the experimental studies based on the SV waves observed at Japanese stations.

Further analyses are made here by using the amplitude ratio and phase difference between SH waves and the horizontal component of SV waves, since SH waves contain different kind of information on a layered structure from that of SV waves. The main purpose of the present paper is to test the appropriateness of probable crust-mantle models derived from P wave spectrum and also from other sources of information such as travel times of body waves from explosions or earthquakes, dispersion of surface waves or gravity anomalies, and to select a model best approximate to the structure under consideration. It is also well known that the observed phase velocities of both Love and Rayleigh waves cannot be explained by a single isotropic

* Now at Seismological Laboratory, California Institute of Technology, Pasadena, California 91109.

layered model, and two different mantle models, anisotropic and laminated models, have been presented to account for the discrepancy. It is expected that a combined analysis of SH and SV waves by the present method might give another approach to the problem.

## §2. Data and Method of Analysis

The method described above is applied to the crust-mantle structure around three Japanese stations, Tsukuba (TSK) in the Kwanto Plain, Matsushiro (MAT) in the central mountain area and Shiraki (SHK) in the Chugoku region, and two U.S. stations, Albuquerque (ALQ) in the mid-continent of New Mexico and Bermuda (BEC), Columbia, on the Atlantic Ocean, where the structures have been estimated from the spectral study of long-period P waves (KURITA, 1969a, b; 1970; PHINNEY, 1964). The locations of the stations are listed in Table 1.

Data used are the two long-period horizontal component seismograms recorded at the above stations; the instruments operated at TSK are the Columbia seismographs similar to those of the Press-Ewing type, while those at the other four stations have the conventional system used at the WWSSN. Table 2 tabulates the earthquakes analyzed for the respective stations, with their relevant information. Theoretical considerations made in Part 1 indicate that it is desirable to select S wave records from deep-focus earthquakes in the epicentral distances between 40° and 60°, in order to obtain reliable spectrum of direct S waves free from contamination by preceding and later phases and from distortion due to large incident angles such that $c<\alpha_n$. It was rather difficult to select many good records of S waves that satisfy the requirements. Although some of the earthquakes listed in the above table do not satisfy the conditions, particular attention was paid in those cases to exclude the effects of later phases.

The technique of analysis employed is as described in Part 1. The two horizontal (NS and EW) records of S waves were digitized at time intervals of 0.7–1.4 sec and resolved into SH waves and horizontal SV waves. A power data window with $n=10\sim20$ (KURITA, 1969a) was then applied to the resolved signals, with its center around the wave group having maximum energy. The amplitude and phase spectra of the two types of S waves have been computed by the Fourier transform of the windowed records. The amplitude ratio and the phase difference between SH waves and the horizontal component of SV waves reduce to (KURITA and MIKUMO, 1971),

$$A_{SH}(\omega)/A_{SV_u}(\omega)=\tan\varepsilon\cdot A_{C\text{-}SH}(\omega)/A_{C\text{-}SV_u}(\omega)$$

and

$$P_{SH}(\omega)-P_{SV_u}(\omega)=P_{C\text{-}SH}(\omega)-P_{C\text{-}SV_u}(\omega)+2n\pi\ ,$$

since the source function, source crust-mantle transfer function, mantle transfer function, and the instrumental response, which are to be involved in the observed spectrum of both types of waves, have been dropped. These relations enable us to compare the S wave observations directly with the functions associated with the crust-mantle structure, with some allowance to $\tan\varepsilon$, the polarization angle of S waves, and to $2n\pi$ ($n$ is an integer). Theoretical functions in the right-hand side are computed by the Thomson-Haskell matrix method (HASKELL, 1962) over the frequency range from 0.01 to 0.25 c/s for appropriate angle of incidence to the models described below.

Table 1. Location of recording stations.

| Station | Code | Latitude | Longitude | Height |
|---|---|---|---|---|
| Tsukuba | TSK | 36° 12′ 39.0″ N | 140° 06′ 36.0″ E | 286 m |
| Matsushiro | MAT | 36 32 30.0 | 138 12 32.0 | 440 |
| Shiraki | SHK | 34 31 56.0 | 132 40 39.0 | 285 |
| Albuquerque | ALQ | 34 56 30.0 | 106 27 30.0 W | 1853 |
| Bermuda | BEC | 32 22 46.0 | 64 40 52.0 | 41 |

## § 3. Inferences of Crust-Mantle Structure from SH and SV Waves

### 1. *Japanese Stations*

Examples of the seismograms analyzed for three Japanese stations are shown in Fig. 1. The epicentral distances and incident angles to these stations, and the time interval of analysis are given in Table 2.

(1) Tsukuba (TSK)

Two deep-focus earthquakes were analyzed. The observational functions for shocks SE 26 in the southeast and SW 18 in the southwest directions are shown in Figs. 2(a) and 2(b). For the structure in the region southeast of TSK, KURITA (1969b) gave seven models designated as SE-A, B, C, D, E, F and G, and four models SW-A, D, F and G, for the southwest region which were able to explain, to some extent, the spectral behaviors of observed P waves. The theoretical functions of S waves have been computed for all of these models, but each three of them are given in the above figures. Comparison of the theoretical curves with the observations indicates that model SE-A seems to give the best fit in the positions of peaks and troughs both for the amplitude ratio and phase difference over frequencies between 0.02 and 0.18 c/s, although the relative heights of the peaks differ for the two types of curves. It also appears that there is no reason to exclude model SE-B in

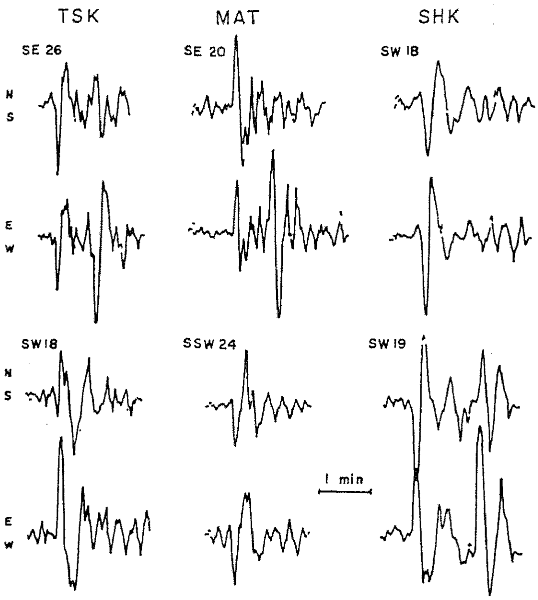


Fig. 1. Seismograms of S waves recorded at three Japanese stations.

Table 2. Information of the earthquakes analyzed in this study.

| No. | Shock | Origin Time | Location | Depth | $\Delta$ | $i_m$ | $\varphi$ | $T_l$ |
|---|---|---|---|---|---|---|---|---|
| 1 | TSK SE 26<br>MAT SE 20<br>SHK SE 5 | Jan. 24, 1969<br>02 33 03.5 | 21.9 S 179.6 W | 595km | 69°.2<br>70.5<br>72.1 | 35°<br>25<br>24 | 140°.0<br>138.5<br>133.8 | 32<br>54<br>38 |
| 2 | TSK SW 18<br>MAT SSW 24<br>SHK SW 18 | Mar. 24, 1967<br>09 00 19.5 | 6.0 S 112.4 E | 600 | 49.4<br>48.7<br>44.6 | 31<br>31<br>33 | 217.6<br>215.3<br>209.5 | 50<br>60<br>50 |
| 3 | SHK SW 19 | May 21, 1967<br>18 45 11.7 | 1.0 S 101.5 E | 173 | 45.9 | 33 | 226.2 | 48 |
| 4 | ALQ (2)<br>BEC (1) | Aug. 28, 1962<br>10 59 59.0 | 38.0 N 23.1 E | 120 | 93.7<br>69.4 | 20<br>27 | 38.0<br>58.0 | 39<br>27 |
| 5 | ALQ (4)<br>BEC (2) | Nov. 3, 1965<br>01 39 02.5 | 9.1 S 71.4 W | 583 | 54.9<br>41.7 | 27<br>33 | 136.0<br>190.0 | 36<br>36 |
| 6 | ALQ (1) | May 22, 1962<br>08 06 38.7 | 12.3 S 166.6 W | 151 | 94.5 | 20 | 258.0 | 45 |
| 7 | ALQ (3) | May 1, 1963<br>10 03 20.0 | 19.0 S 169.0 W | 140 | 96.4 | 19 | 251.0 | 58 |

$\Delta$; epicentral distance, $\varphi$; back azimuth, $i_m$; incident angle to the Moho,
$T_l$; time interval of analysis (sec).

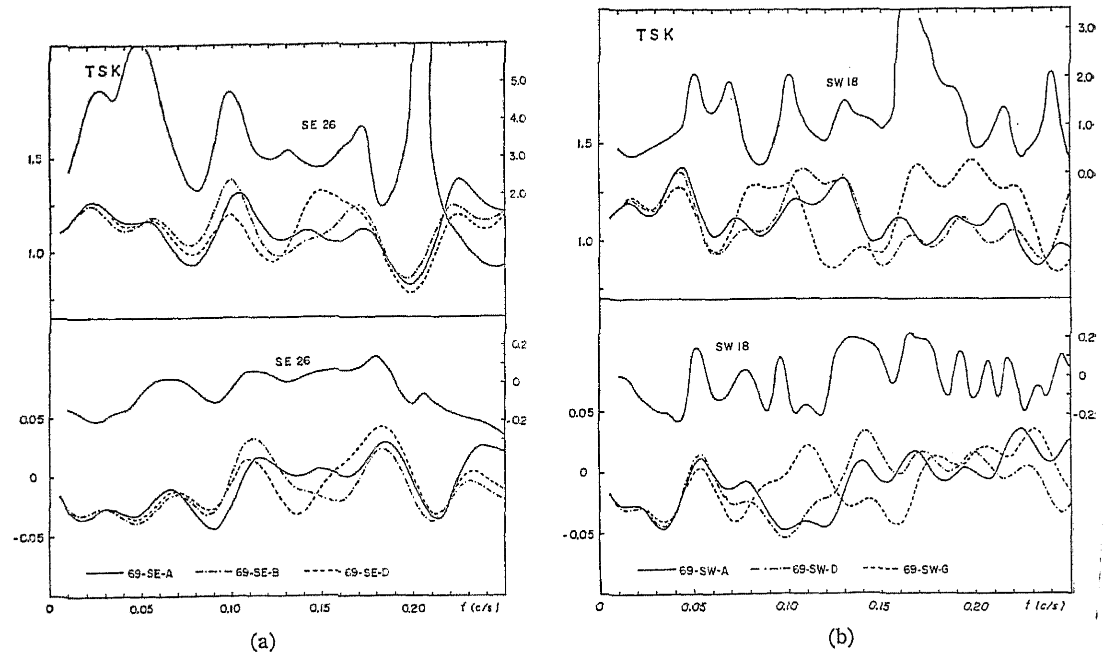


Fig. 2. Observational and theoretical amplitude ratios (upper) and phase differences (lower) between SH and SV waves.
(a) for the southeast region of TSK. (b) for the southwest region of TSK.

view of the degree of fit. It has been stated in the analysis of P wave spectra (KURITA, 1969b) that the first four of the seven models, particularly model SE-A among them, seem to be most probable structures around TSK. The spectra of S waves are consistent with the above inferences. The crustal thickness of 28-30 km in model SE-A as well as in B, C, or D is in good agreement with that for the southeast Kwanto region estimated from explosion studies, dispersion of Rayleigh waves and gravity anomalies (MIKUMO, 1969), *although the layer configurations are somewhat different*. The spectrum of both P and S waves suggests that there may be a rather thick intermediate layer with a compressional velocity around 7.4 km/sec in this region. The thickness estimated in any of the four models exceeds Mikumo's estimation and rather close to Kanamori's inference from Rayleigh waves (1963). For the southwest region, model SW-A appears to be somewhat better than the others, but with a lower degree of fit. Although this model has been selected also from P wave spectrum, its thin crust and a very thick intermediate layer do not agree with the previous results from explosions and Rayleigh waves.

(2) Matsushiro (MAT)

For this station, two deep-focus earthquakes SE 20 and SSW 24 were analyzed. Figs. 3(a) and 3(b) give the results of analysis for the two shocks respectively. The observational functions for SE 20 do not seem to have a high quality, due to the existence of rather short periods in the original records. The theoretical functions to be compared with the observations are those for model SE-A, B, C and D and SSW-A, B, C and D respectively (KURITA, 1971). None of the theoretical curves can explain satisfactorily the observational curves for SE 20, showing only a poor fit in the case of model SE-B or A. It can be seen, however, that the positions of peaks and troughs for model SSW-B, except for frequencies lower than 0.04 c/s, agree quite well with those of the observations for SSW 24, particularly in the amplitude ratio curve. Model SSW-D follows B in the degree of fit. KURITA (1971) has also suggested in the

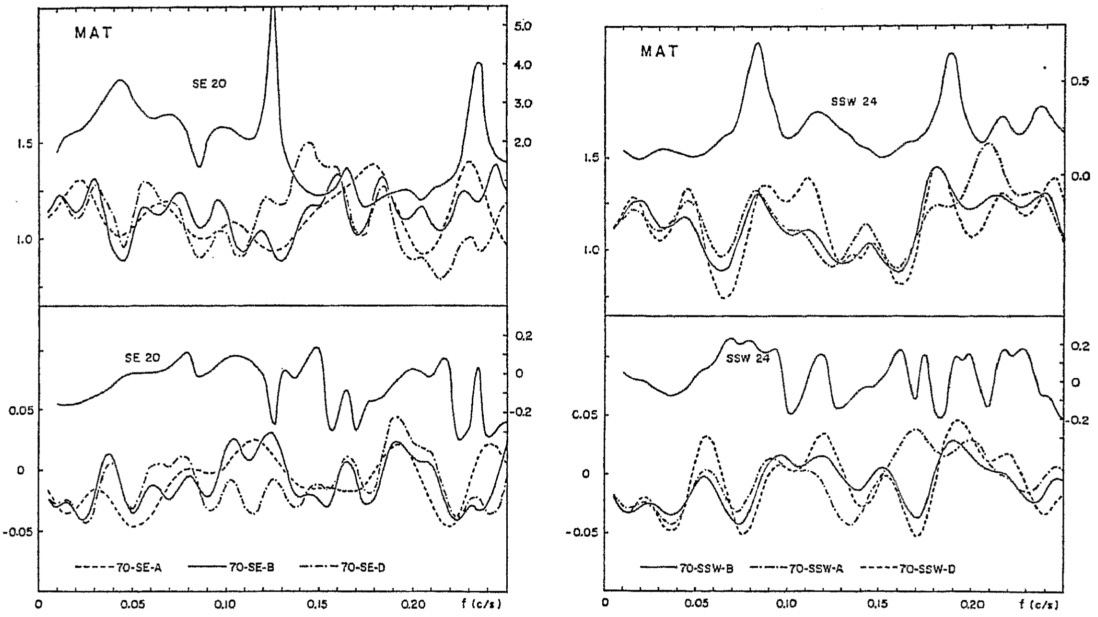


(a) (b)

Fig. 3. Observational and theoretical amplitude rations (upper) and phase differences (lower) between SH and SV waves.
(a) for the southeast region of MAT. (b) for the southwest region of MAT.

spectral study of P waves that the most probable structure in the region southwest of Matsushiro may be model SSW-B or A. The thickness down to the boundary between the lower crust (6.8 km/sec) and the intermediate layer (7.4 km/sec) is about 36 km in model SSW-B, and this is in close agreement with the results for this region estimated from explosions and gravity anomalies (MIKUMO, 1966). The observations of P and S waves appear to support the existence of a thick intermediate layer in this region. If we take this interpretation, however, the layer will be much thicker than previously considered, although there might be some lateral difference in the thickness. Another possibility of a thick lower crust instead of the intermediate layer as supposed in model SSW-D cannot be ruled out. If this is true, the crustal thickness would be about 60 km, which compares with the corresponding total thickness of 64 km in model SSW-B.

(3) Shiraki (SHK)

Two deep-focus and an intermediate earthquakes were analyzed, but the results given

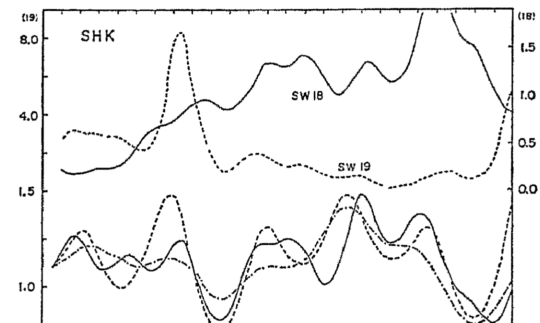


Fig. 4. Observational and theoretical amplitude ratios (upper) and phase differences (lower) between SH and SV waves for the southwest region of SHK.

in Fig. 4 are for two shocks in the southwest direction. The general form of the observational functions differs appreciably for shock SW-18 (deep) and SW-19 (intermediate), but a close examination shows agreement between the two shocks in the positions of peaks and troughs for frequencies between 0.10 and 0.22 c/s. The other shock SE-5 in the southeast direction indicates peaks at 0.055 and 0.155 c/s and troughs at 0.10 and 0.19 c/s. The difference in the features from the first two shocks may be due to a shorter time interval of analysis, and the results have not been taken into later considerations. The theoretical functions of SH and SV waves for four probable models 70-1, 2, 3 and 4 (KURITA, 1970) are plotted in the above figure. Comparing these theoretical curves with the observations for frequencies from 0.07 to 0.21 c/s, we may say that model 70-4 gives a satisfactory agreement among the four models, as has been suggested from the P and SV wave spectra (KURITA, 1970, 1971), but that models 70-2 and 3 cannot be rejected. The structure of model 4 with a crustal thickness of 41 km and a thick intermediate layer differ considerably from any previously proposed models from explosions and surface waves, while model 2 is similar to one of the models presented by MIKUMO (1966) and the model of KANAMORI (1963) for western Japan, and model 3 is close to Model II derived from explosion observations near this region (HASHIZUME *et al.*, 1966).

Table 3. Crust-mantle models for three regions of Japan‡

| Model | | 1 | 2 | 3 | 4 | M | Fit |
|---|---|---|---|---|---|---|---|
| TSK 69 | α(km/sec) | 5.50 | 6.05 | 6.60 | 7.40 | 8.00 | |
| | β(km/sec) | 3.10 | 3.40 | 3.70 | 4.15 | 4.50 | |
| | ρ(g/cm³) | 2.50 | 2.65 | 2.85 | 3.10 | 3.30 | |
| *SE -A | H(km) | 5 | 15 | 8 | 23 | — | A |
| SE -B | | 5 | 3 | 22 | 23 | — | B |
| SE -D | | 5 | 13 | 12 | 21 | — | C |
| SW-A | | 5 | 9 | 7 | 54 | — | B |
| SW-D | | 5 | 13 | 6 | 48 | — | B |
| SW-G | | 5 | 8 | 17 | 40 | — | C |
| MAT 70 | α(km/sec) | 4.40 | 6.05 | 6.80 | 7.35 | 8.00 | |
| | β(km/cec) | 2.55 | 3.40 | 3.80 | 4.10 | 4.50 | |
| | ρ(g/cm³) | 2.50 | 2.70 | 2.90 | 3.05 | 3.30 | |
| SE -A | H(km) | 1 | 27 | 9 | 10 | — | |
| SE -B | | 1 | 28 | 15 | 54 | — | C |
| SE -D | | 1 | 16 | 30 | 52 | — | |
| SSW-A | | 1 | 11 | 22 | 33 | — | C |
| *SSW-B | | 1 | 26 | 9 | 27 | — | A |
| SSW-D | | 1 | 26 | 33 | 0 | — | B |
| SHK 70 | α(km/sec) | 5.50 | 6.05 | 6.50 | 7.40 | 8.00 | |
| | β(km/sec) | 3.10 | 3.40 | 3.65 | 4.15 | 4.50 | |
| | ρ(g/cm³) | 2.50 | 2.70 | 2.80 | 3.10 | 3.30 | |
| 1 | H(km) | 3 | 7 | 6 | 31 | — | C |
| 2 | | 3 | 12 | 11 | 17 | — | C |
| 3 | | 3 | 7 | 32 | 0 | — | B |
| * 4 | | 3 | 12 | 26 | 26 | — | A |

‡ taken from Kurita (1969a, b, 1970, 1971).

The layer parameters in all probable models for the three regions are given in Table 3. The "Fit" implies the degree of fit between the observational and theoretical functions of S waves, and an asterisk indicates the most probable model for each region. The features of the preferred structures will be discussed later.

## 2. *U.S. Stations*

The seismograms of S waves recorded at two U.S. stations, Albuquerque and Bermuda are shown in Fig. 5, and their pertinent information is given in Table 2.

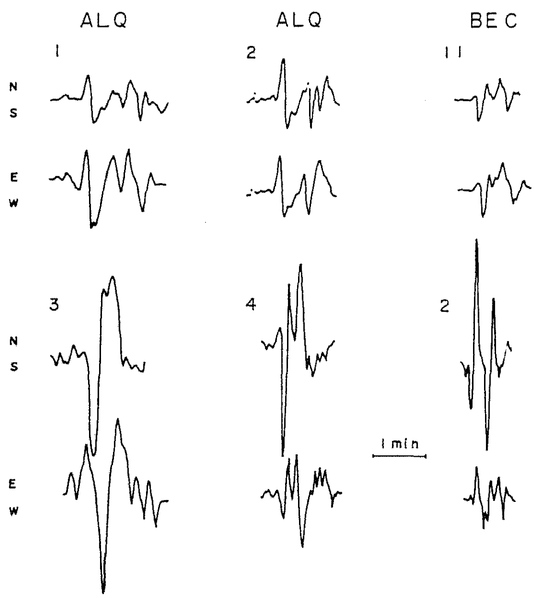


Fig. 5. Seismograms of S waves recorded at two U. S. stations.

(1) Albuquerque (ALQ)

Three intermediate-depth and a deep-focus earthquakes were analyzed. The results of analysis are grouped into those for shocks (1) and (4) and for shocks (2) and (3), according to the positions of peaks and troughs in the observational functions, but do not seem to be related to the direction of wave approach, incident angle or recorded waveforms. PHINNEY (1964) gave a number of possible crustal models for this region to explain the spectral behaviors of P waves. The theoretical functions of SH and SV waves have been computed here for seven models, THL-12 and 13; PRM-3, 6, 15 and 21; and VEL-6, for which the degree of fit with P wave observations was highly ranked as A. Fig. 6(a) gives the observational curves for the first group together with the theoretical functions for the above models except PRM-6. As may be seen from the figure, model THL-12 fits well with the observational curves, particularly of the amplitude ratio for shock (1), and models VEL-6 and PRM-3 are also able to yield a fairly satisfactory agreement with the observations either for shock (1) or (4). However, the observational functions shown in Fig. 6(b) for the second group cannot be explained by any models mentioned here. The reason for this remains unsolved at this time.

Model THL-12 has a typical double-layered continental crust with a thickness of 35 km, while models PRM-3 and VEL-6 have a transitional layer, and the depth to the base of the lower crust is 36-38 km. Thus, the spectrum of S waves in some cases appears consistent with PHINNEY's inferences (1964) on the crustal thickness under Albuquerque. There leaves a possibility, however, that the structure includes an intermediate layer with a compressional velocity of 7.5-7.6 km/sec and a thickness of several km.

(2) Bermuda (BEC)

A deep-focus and an intermediate earthquakes were analyzed. The observational functions for two shocks (1) and (2) are shown in Fig. 7, indicating gentle variations with frequency as compared with those for the other stations. The positions of peaks and troughs agree for the two shocks over frequencies between 0.07 and 0.21 c/s. The corresponding theoretical functions have been

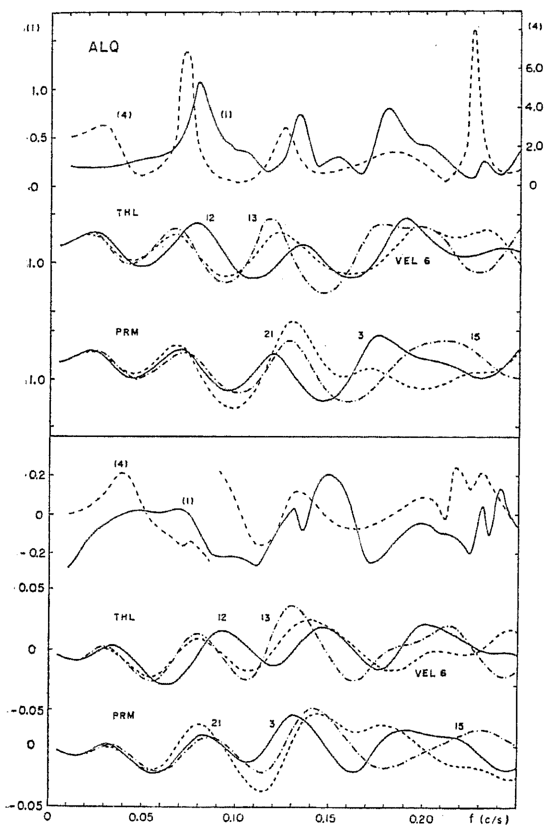

(a)

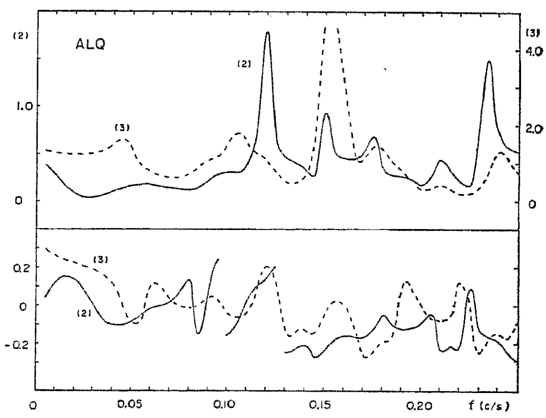

(b)

Fig. 6. Observational and theoretical amplitude ratios (upper) and phase differences (lower) between SH and SV waves for the region around ALQ.
(a) for the first group. (b) for the second group.

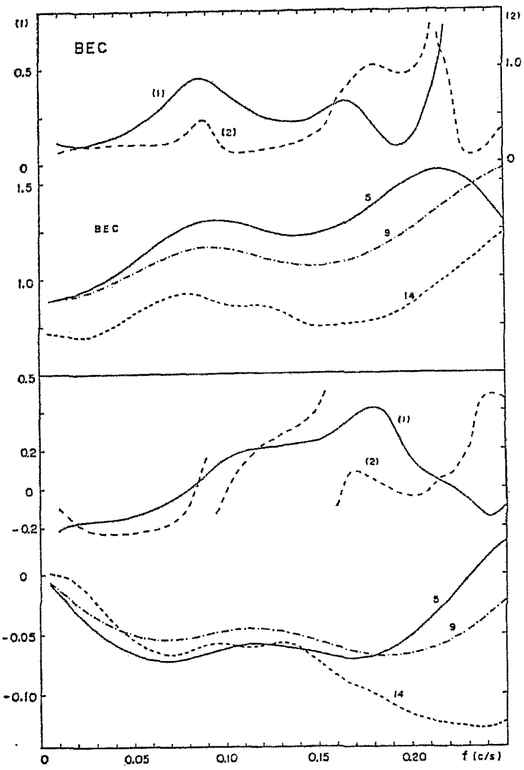


Fig. 7. Observational and theoretical amplitude ratios (upper) and phase differences between SH and SV waves for the region around BEC.

computed for the six models numbered as 5, 9, 11, 14, 17 and 18 with an oceanic crust, which fit reasonably well the P wave spectrum (PHINNEY, 1964), but three of them are given in the above figure. Comparison in Fig. 7 shows that model 5 yields a satisfactory agreement with the observations in the positions of the first peak and the first trough both in the amplitude ratio and the phase difference curves. For frequencies higher than 0.18 c/s this model explains only the general trend of the observations for shock (2). It seems that model 9 follows model 5. The other models including model 14 do not fit the observations. Models 5 and 9 have a thickness of 12 km for the substantial crustal layer. It is not certain, however, whether there is a 5.4 km/sec surface layer or not, in view of less reliable behaviors of the observational curves for high frequencies.

Table 4. Crust-mantle models for two regions of the United States*

| Model | | 1 | 2 | 3 | 4 | 5 | Fit |
|---|---|---|---|---|---|---|---|
| ALQ THL | $\alpha$(km/sec) | 6.14 | 6.80 | 8.10 | | | |
| | $\beta$(km/sec) | 3.50 | 3.85 | 4.55 | | | |
| | $\rho$(gr/cm$^3$) | 2.75 | 2.95 | 3.32 | | | |
| -12 | $H$(km) | 25 | 10 | — | | | A |
| -13 | | 25 | 15 | — | | | B |
| PRM | $\alpha$(km/sec) | 6.14 | 6.70 | 7.60 | 8.10 | | |
| | $\beta$(km/sec) | 3.50 | 3.80 | 4.30 | 4.50 | | |
| | $\rho$(gr/cm$^3$) | 2.91 | 3.14 | 3.20 | 3.35 | | |
| - 3 | $H$(km) | 26 | 12.5 | 1.0 | — | | C |
| - 6 | | 26 | 9.5 | 3.5 | — | | C |
| -15 | | 22.5 | 13.0 | 3.5 | — | | C |
| -21 | | 18 | 20.5 | 0.5 | — | | B |
| VEL | $\alpha$(km/sec) | 6.14 | 6.58 | 7.45 | 8.10 | | |
| | $\beta$(km/sec) | 3.50 | 3.67 | 4.17 | 4.50 | | |
| | $\rho$(gr/cm$^3$) | 2.91 | 3.14 | 3.20 | 3.35 | | |
| - 6 | $H$(km) | 22.5 | 13.0 | 7.5 | — | | A |
| BEC A | $\alpha$(km/sec) | 5.43 | 6.81 | 8.10 | 8.00 | 7.90 | |
| | $\beta$(km/sec) | 3.15 | 3.90 | 4.55 | 4.45 | 4.35 | |
| | $\rho$(gr/cm$^3$) | 2.70 | 2.95 | 3.33 | 3.30 | 3.30 | |
| - 5 | $H$(km) | 5.0 | 7.0 | — | | | A |
| - 9 | | 0.0 | 12.0 | — | | | B |
| -11 | | 0.0 | 12.0 | 13.0 | 20.0 | — | C |
| -14 | | 0.0 | 12.0 | 28.0 | 20.0 | — | C |
| B | $\alpha$(km/sec) | 5.43 | 6.81 | 8.40 | | | |
| | $\beta$(km/sec) | 3.15 | 3.90 | 4.50 | | | |
| | $\rho$(gr/cm$^3$) | 2.70 | 2.95 | 3.33 | | | |
| -18 | $H$(km) | 5.0 | 7.0 | — | | | C |
| C | $\alpha$(km/sec) | 5.43 | 6.65 | 8.10 | | | |
| | $\beta$(km/sec) | 3.15 | 3.80 | 4.55 | | | |
| | $\rho$(gr/cm$^3$) | 2.70 | 2.95 | 3.33 | | | |
| -17 | $H$(km) | 5.0 | 7.0 | — | | | B |

* taken from Phinney (1964).

All of the probable models discribed above are tabulated in Table 4, together with the degree of fit between the observational and theoretical functions of S waves.

## 3. *Discussion*

The S wave data we have tentatively analyzed are from only a few earthquakes for each station. It is undoubtedly necessary to analyze much more data before any definite conclusions can be drawn on the structures. Nevertheless, a limited number of reliable data appears to suggest that the spectra of

SH and SV waves are generally consistent with some of the structures inferred from P wave spectrum, and also with the average crustal thickness derived from explosions, Rayleigh waves and gravity anomalies. There are some differences, however, in the information from these methods about the lower crust or the intermediate layer. The differences probably reflect the advantages or disadvantages inherent to these methods.

A remarkable feature of the structures in Japan revealed by the body wave spectrum is that there appears to be a thick intermediate layer with velocities between those appropriate to the lower crust and the normal upper mantle. Also, the spectrum shows characteristic difference between the continental and oceanic crusts in selected two regions of North America, although detailed layer configurations cannot be determined. It is interesting to note that there is a possibility that a thin intermediate layer might exist between the lower part of the continental crust and the upper mantle, but the thickness does not compare with the structure in Japan even if it exists. A hypothesis might be drawn that in tectonically active regions such as Japan Islands, Basin and Range Province in North America, the western part of South America and several island arcs, the lower crust would change over some range of depths to the normal mantle, as characterized by a rather low Pn velocity or the existence of an intermediate layer, while in stable continental regions the transition would be rather abrupt. However, this hypothesis is only speculative and has to be tested by other evidence.

## § 4. Some Considerations on Dispersion of Surface Waves and Spectrum of S waves in Anisotropic and Laminated Mantle Models

The structures in the regions around Matsushiro and Tsukuba have been estimated not only from travel times of explosions, gravity

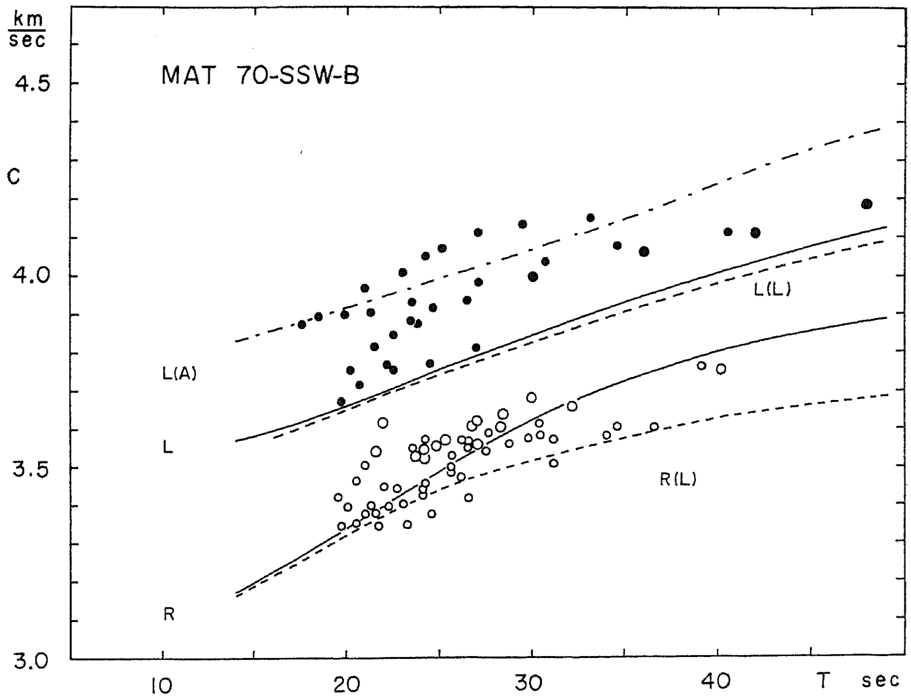


Fig. 8. Observed and computed phase velocities of Love and Rayleigh waves for MAT. R: Rayleigh waves, L: Love waves, (L) laminated model, (A): anisotropic model.

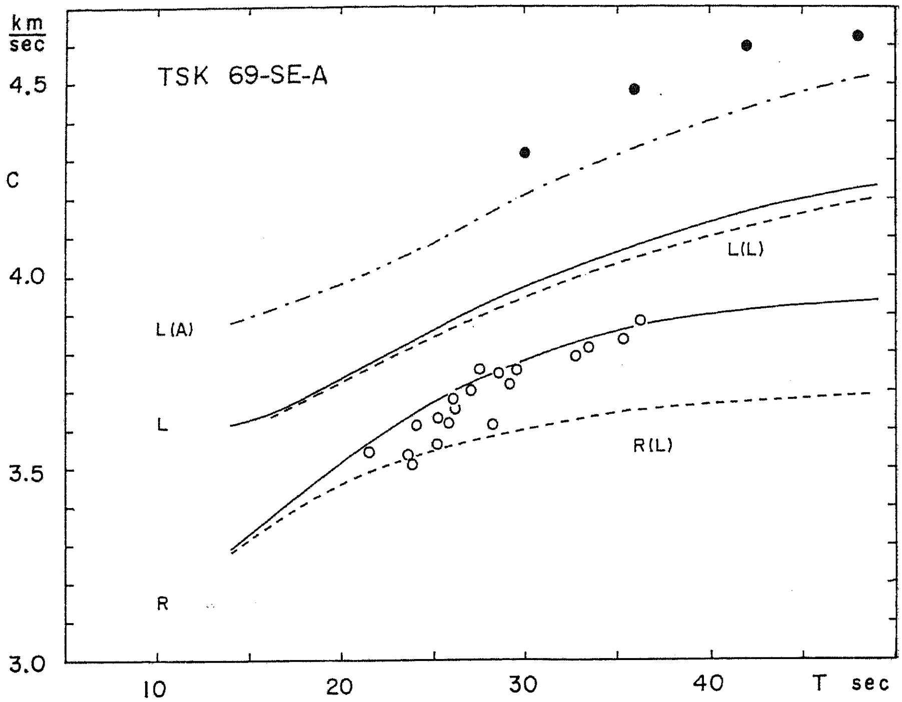


Fig. 9. Observed and computed phase velocities of Love and Raleigh waves for TSK.

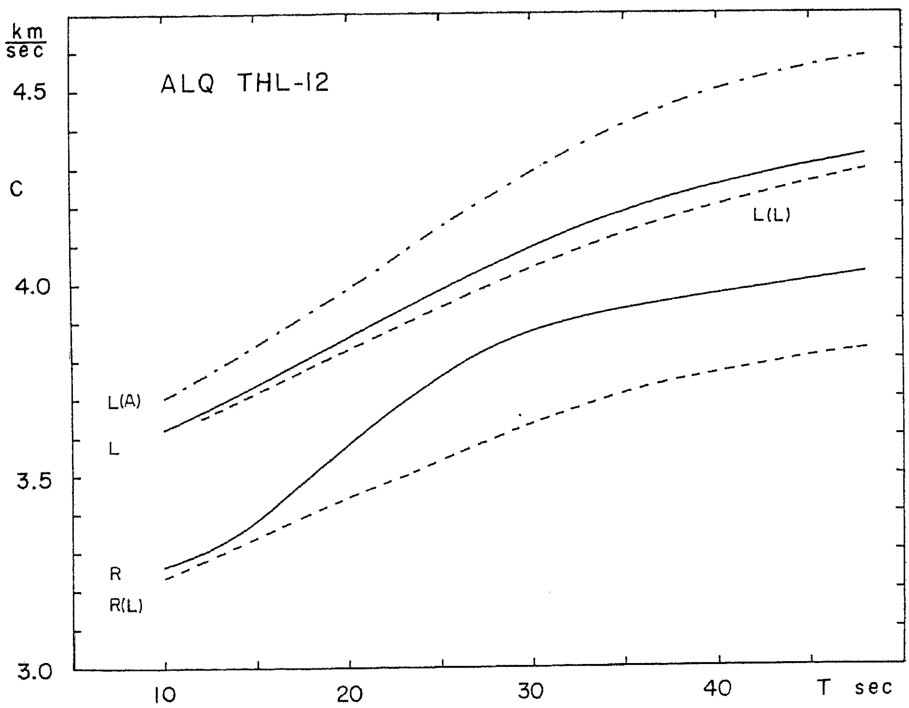


Fig. 10. Computed phase velocities of Love and Rayleigh waves for ALQ.

anomalies but from dispersion of Rayleigh waves (MIKUMO, 1966). The spectral study of SH and SV waves, as well as of P waves (KURITA, 1969a, b, 1970), suggests, however, a much thicker intermediate layer than previously derived. For this reason, the dispersions of both Rayleigh and Love waves are re-investigated here to see if they are consistent with the above evidence.

The observed phase velocities for central and eastern Japan were taken from AKI (1961), AKI and KAMINUMA (1963), and KAMINUMA (1966). The open and solid circles plotted in Figs. 8 and 9 indicate those of Rayleigh and Love waves, and large and small ones are from the array technique, and from the interval velocities which were not included in the previous work. Theoretical phase velocities of Rayleigh and Love waves have been computed here by the Thomson Haskell matrix method (HASKELL, 1953) for the preferred models in the foregoing section; MAT SSW-B for the region near Matsushiro, TSK SE-A for Tsukuba, and ALQ THL-12, respectively, and are indicated by R and L in the figures. It is evident in Figs. 8 and 9 that these models can explain satisfactorily the observed phase velocities of Rayleigh waves in the two regions, while the observed velocities of Love waves are significantly higher than the theoretically expected values.

This type of inconsistency between Love and Rayleigh wave dispersion has been discussed by AKI and KAMINUMA (1963) and KAMINUMA (1966a) for central Japan, by MCEVILLY (1964) for the mid-continent of the United States, and also by SAITO and TAKEUCHI (1966) for marginal zones between continents and oceans. To date, three different interpretations have been presented to account for the inconsistency. MCEVILLY (1964) and KAMINUMA (1966b) explained the discrepancy by a simplified anisotropic (transversely isotropic) model, assuming that the SH wave velocity in the upper mantle is 7–8% higher than that of SV waves. On the other hand, AKI (1968) proposed a laminated mantle model with thin soft layers interleaved alternatively in horizontal layers of hard materials, and concluded that 2% soft layers with a shear velocity of 1.1 km/sec would be enough to reconcile the discrepancy. HALES and BLOCH (1969) also suggested a laminated mantle for the United States. TAKEUCHI *et al.* (1968) presented a model that includes elliptical magma pockets, which reduces the velocity of Rayleigh waves but remains that of Love waves almost unchanged. The other interpretation is that anomalous Love wave velocities are the results of higher mode interference to the fundamental mode (THATCHER and BRUNE, 1969). However, there is an argument (BOORE, 1969) against this interpretation, stating that no uniform bias occurs from contaminations in the velocities measured from an emsemble of earthquakes. It has been demonstrated (BACKUS, 1962) that for long waves a laminated model becomes equivalent to a transversely isotropic medium, but there might be some differences between them for the wavelength with which we are concerned, since the long wave restriction is quite severe (ANDERSON, 1962). For this reason, we shall examine here not only the dispersion of surface waves but the spectral behaviors of SH and SV waves in both laminated models and transversely isotropic models based on the preferred structure.

(*1*) *Laminated models*

We computed the phase velocities of Love and Rayleigh waves for the three laminated mantle models given in Table 5, in which four or five layers of soft material (the fraction being 1.2–1.5%) with a thickness of 0.2 km/sec and with a shear velocity as low as 1.1 km/sec (AKI, 1968) are interleaved in models MAT SSW-B, TSK SE-A and ALQ THL-12, respectively. The computed phase velocities are shown by L(L) and R(L) in Figs. 8, 9 and 10. It can be seen that Love wave velocities fall by less than 1% from the isotropic case while for Rayleigh waves the drop reaches about 6% at 40 sec. For both types of waves, the theoretical velocities for the laminated models as given here tend to deviate from the observations at MAT and TSK. However, if we assume a laminated model as applied to ALQ for Matsushiro, which does not include an intermediate layer, both the Love and Rayleigh wave observations can be explained satisfactorily. It is still unable to explain by this model the Love wave observations at Tsukuba. The above discrepancy between the two types of waves would also be explained by the model of TAKEUCHI *et al.* (1968).

Table 5. Laminated mantle models.

1. MODEL MAT 70 SSW-B

| $\alpha$ | $\beta$ | $\rho$ | $H$ |
|---|---|---|---|
| 4.40 | 2.55 | 2.50 | 1.0 |
| 6.05 | 3.40 | 2.70 | 26.0 |
| 6.80 | 3.80 | 2.90 | 9.0 |
| 7.35 | 4.10 | 3.05 | 27.0 |
| 7.35 | 1.00 | 3.10 | 0.2 |
| 8.00 | 4.50 | 3.30 | 10.0 |
| 7.35 | 1.00 | 3.10 | 0.2 |
| 8.00 | 4.50 | 3.30 | 10.0 |
| 7.35 | 1.00 | 3.10 | 0.2 |
| 8.00 | 4.50 | 3.30 | 10.0 |
| 7.35 | 1.00 | 3.10 | 0.2 |
| 8.00 | 4.50 | 3.30 | |

2. MODEL TSK 69 SE-A

| $\alpha$ | $\beta$ | $\rho$ | $H$ |
|---|---|---|---|
| 5.50 | 3.10 | 2.50 | 5.0 |
| 6.05 | 3.40 | 2.65 | 15.0 |
| 6.60 | 3.70 | 2.85 | 8.0 |
| 7.40 | 4.15 | 3.10 | 23.0 |
| 7.40 | 1.00 | 3.10 | 0.2 |
| 8.00 | 4.50 | 3.30 | 10.0 |
| 7.40 | 1.00 | 3.10 | 0.2 |
| 8.00 | 4.50 | 3.30 | 10.0 |
| 7.40 | 1.00 | 3.10 | 0.2 |
| 8.00 | 4.50 | 3.30 | 10.0 |
| 7.40 | 1.00 | 3.10 | 0.2 |
| 8.00 | 4.50 | 3.30 | |

3. ALQ THL-12

| $\alpha$ | $\beta$ | $\rho$ | $H$ |
|---|---|---|---|
| 6.14 | 3.50 | 2.75 | 25.0 |
| 6.80 | 3.85 | 2.95 | 10.0 |
| 7.50 | 1.10 | 3.20 | 0.2 |
| 8.10 | 4.55 | 3.32 | 10.0 |
| 7.50 | 1.10 | 3.20 | 0.2 |
| 8.10 | 4.55 | 3.32 | 10.0 |
| 7.50 | 1.10 | 3.20 | 0.2 |
| 8.10 | 4.55 | 3.32 | 10.0 |
| 7.50 | 1.10 | 3.20 | 0.2 |
| 8.10 | 4.55 | 3.32 | 10.0 |
| 7.50 | 1.10 | 3.20 | 0.2 |
| 8.10 | 4.55 | 3.32 | |

$\alpha$ in km/sec, $\beta$ in km/sec, $\rho$ in gr/cm$^3$, $H$ in km.

The theoretical amplitude ratios and phase differences between SH and SV waves for the above laminated mantle models in the three regions are given as L in Figs. 11, 12 and 13. It is evident from the figures that the positions of peaks and troughs differ appreciably from those for the isotropic case which fits well the observations. A laminated model such as ALQ THL-12 does not argee also with the isotropic case and hence with the observations at the two stations. This implies that the laminated models given above are not supported by the observed spectra of SH and SV waves, although some of the models were able to reconcile the inconsistency between the observed phase velocities of Love and Rayleigh waves.

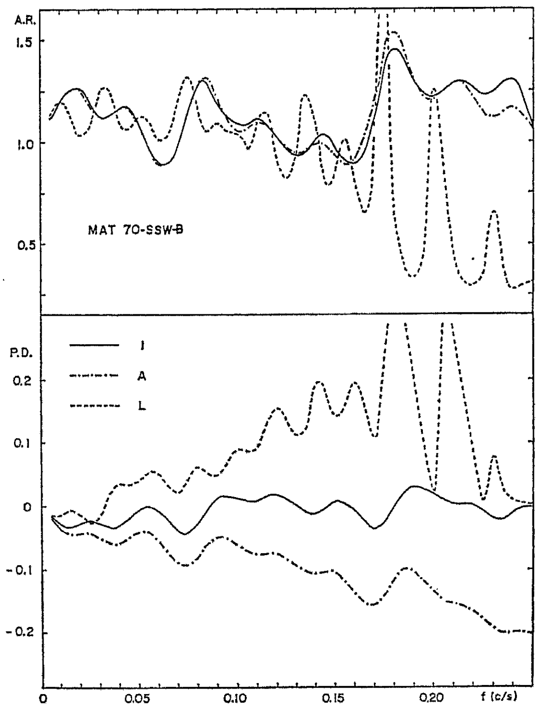


Fig. 11. Theoretical amplitude ratios (upper) and phase differences (lower) for model MAT SSW-B. I: isotropic model, L: laminated model, A: anisotropic (transversely isotropic) model.

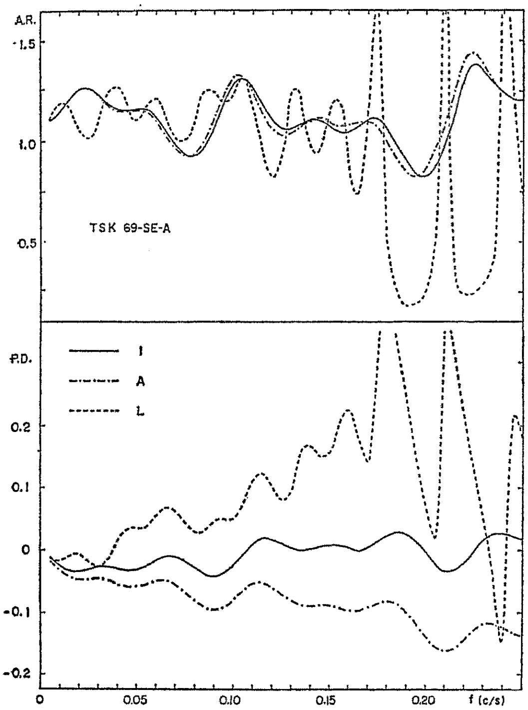


Fig. 12. Theoretical amplitude ratios and phase differences for model TSK SE-A.

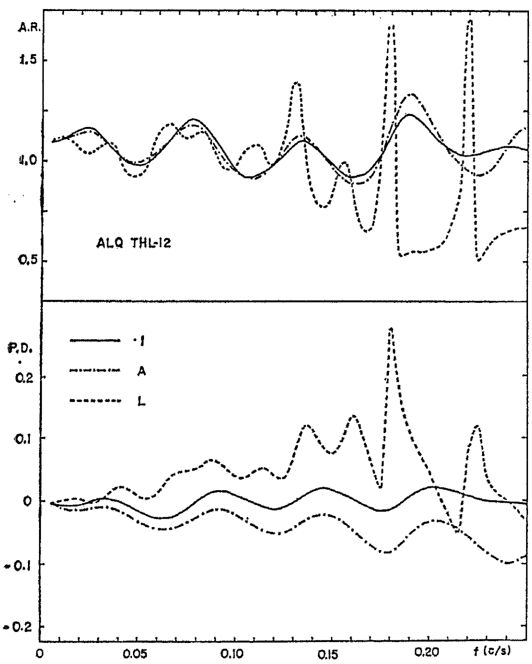


Fig. 13. Theoretical amplitude ratios and phase differences for model ALQ THL-12.

(2) *Anisotropic (transversely isotropic) models*

Dispersion of surface waves in a layered transversely isotropic medium has been discussed by ANDERSON (1961, 1962) and HARKRIDER and ANDERSON (1962). In the medium there is no coupling between motions of Rayleigh and Love waves (ANDERSON, 1961), and hence the phase velocity of Rayleigh waves is not affected by SH wave velocity. KAMINUMA (1966b) has computed Love wave dispersion for a two-layer model in central Japan on the basis of ANDERSON's formulation (1961).

We calculate here the phase velocity of Love waves and also the crust-mantle transfer function of SH waves for multi-layered transversely isotropic models. Following ANDERSON (1962) and HASKELL (1953, 1960), we have the particle velocity $\dot{v}$ and the tangential stress $p_{zy}$ at the $(n-1)$th interface, in the form,

$$(\dot{v}/c)_{n-1}=A_{11}(\dot{v}/c)_0+A_{12}(p_{zy})_0=ik(v_1+v)_n\,,$$
$$(p_{zy})_{n-1}=A_{21}(\dot{v}/c)_0+A_{22}(p_{zy})_0=ikL_n\zeta_n(-v_1+v_2)_n\,, \quad (1)$$

where $\zeta=(N/L)^{1/2}[(c/\beta_2)^2-1]^{1/2}$, $L=c_{44}=\rho\beta_1^2$, and $N=(c_{11}-c_{12})/2=\rho\beta_2^2$, and $c$ is the phase velocity, $\beta_1$ and $\beta_2$ are the vertical SH velocity or SV velocity and the horizontal SH velocity respectively, and $A_{ij}$ are the elements of layer matrix. The boundary condition at the surface, $(p_{zy})_0=0$ at $z=0$, yields,

$$2v_{2n}=[A_{11}+A_{21}(L_n\zeta_n)^{-1}]v_0\,, \quad (2)$$

where $v_0=(ik)^{-1}(\dot{v}/c)_0$ is the displacement at the surface. For free surface waves with no source in the $n$th layer, $v_{2n}=0$, and hence the Love wave dispersion equation is (ANDERSON, 1962),

$$A_{21}=-A_{11}(L_n\zeta_n)\,. \quad (3)$$

From equation (2), the transfer function of SH waves, or the ratio of the surface amplitude to the incident amplitude, can be written,

$$v_0/v_{2n}=2/[A_{11}+A_{21}(L_n\zeta_n)^{-1}]^{-1}\,. \quad (4)$$

The computations for (3) and (4) were made by putting the pseudo-rigidity $\mu'=(LN)^{1/2}\mu=\rho\beta_1\beta_2$ and the pseudo-layer thickness $d'=(N/L)^{1/2}d=(\beta_2/\beta_1)d$ (ANDERSON, 1962) for each layer into the HASKELL's formulation (1953).

In Figs. 8, 9 and 10 are given by L(A) the phase velocities of Love waves for the three transversely isotropic media modified from models MAT SSW-B, TSK SE-A and ALQ THL-12 respectively, in which we made a tentative assumption that there are 2% anisotropy in the lower crust (KAMINUNA, 1966b) and 8% in the upper mantle (MCEVILLY, 1964). It is found that the computed velocities become large by about 7% than those for the isotropic cases at 30 sec, and hence that they seem slightly higher to fit the observed velocities for MAT (Fig. 8), and still slightly lower for TSK (Fig. 9). The small discrepancies would easily be reconciled by adjusting slightly the assumed anisotropic constant for the two stations, although we did not make further attempts to get a close fit.

The spectral amplitude ratio and the phase difference between SH waves and the horizontal component of SV waves have been computed using equation (4) for the above described transversely isotropic models, and the results for the three regions are given in Figs. 11, 12 and 13. It can be seen directly in all cases that the features of the amplitude ratio curve are close to those of the isotropic case. This is the case for the positions of peaks and troughs of the phase difference curve, although the absolute phase difference tends to be larger than the latter for higher frequencies. A rather wide range of fluctuations of the observed phase difference might be associated with this case.

(3) *Discussion*

There is a critical interpretation (THATCHER and BRUNE, 1969) for Love wave observations that higher mode interference may be the cause of anomalous high velocities. If the high Love wave velocities measured in Japan are not the results of mode interference, the observed discrepancy between Love and Rayleigh waves may be attributed to some departure from homogeneous and isotropic structure. It has been found that either transversely isotropic models or laminated mantle models without the intermediate layer could account for the observations. The spectral behaviors of SH and SV waves are consistent with the transversely isotropic models, whereas they cannot be explained by the laminated models given above. From the above evidence, we prefer the interpretation that there could be some kind of anisotropy in the lower crust, the intermediate layes and the upper mantle, although a transversely isotropy, which is the most simplified form of anisotropy, might not always be met in the mantle. It is interesting to note, however, that there is some evidence that the maximum anisotropy in shear wave velocities reaches 7% for realistic mantle materials such as dunite, peridotite or serpentinite (CHRISTENSEN 1966; KASAHARA *et al.*, 1968) in relation to the preferred orientation of minerals.

**Acknowledgments**

The senior author wishes to thank Dr. Toshikatsu Yoshii and Mr. Akira Sakai for discussion on the present problem, and Mrs. Ritsuko Koizumi for assistance in the present work. The computations involved were made on a FACOM 230-60 at the Data Processing Center, Kyoto University.

**References**

Aki, K., Crustal Structure in Japan from the phase velocity of Rayleigh waves, Part 1. Use of the network of seismological stations operated by the Japan Meteorological Agency, *Bull. Earthq. Res. Inst.*, **39**, 255-283, 1961.

Aki, K. and K. Kaminuma, Phase velocity of Love waves in Japan, Part 1. Love waves from the Aleutian shock of March 9, 1957, *Bull. Earthq. Res. Inst .*, **41**, 243-259, 1963.

Aki, K., Seismological evidences for the existence of soft thin layers in the upper maintle under Japan, *J. Geophys. Res.*, **73**, 585-594, 1968.

Anderson, D. L., Elastic wave propagation in layered anisotropic media, *J. Geophys. Res.*, **66**, 2953-2963, 1961.

Anderson, D. L., Love wave dispersion in heterogeneous anisotropic media, *Geophysics*, **27**, 445-454, 1962.

Backus, G. E., Long-wave elastic anisotropy produced by horizontal layering, *J. Geophys. Res.*, **67**, 4427-4440, 1962.

Boore, D. M., Effect of higher mode contamination on measured Love wave phase velocities, *J. Geophys. Res.*, **74**, 6612-6616, 1969.

Christensen, I., Elasticity of ultrabasic rocks, *J. Geophys. Res.*, **71**, 5921-5931, 1966.

Hales, A. L. and S. Bloch, Upper mantle structure: Are the low velocity layers thin?, *Nature*, **221**, 930, 1969.

Harkrider, D. G. and D. L. Anderson, Computation of surface wave dispersion for multilayered anisotropic media, *Bull. Seism. Soc. Am.*, **52**, 321-331, 1962.

Hashizume, M., O. Kawamoto, S. Asano, I. Muramatu, T. Asada, I. Tamaki and S. Murauchi, Crustal structure in the western part of Japan derived from the observation of the first and second Kurayoshi and Hanabusa explosions, Part 2. Crustal structure in the western part of Japan, *Bull. Earthq. Res. Inst.* **44**, 109-120, 1966.

Haskell, N. A., The dispersion of surface waves on multilayered media, *Bull. Seism. Soc. Am.*, **43**, 17-34, 1953.

Haskell, N. A., Crustal reflection of plane SH waves, *J. Geophys. Res.*, **65**, 4147-4150, 1960.

Haskell, N. A., Crustal reflection of plane P and SV waves, *J. Geophys. Res.*, **67**, 4751-4767, 1962.

Kaminuma, K., The crust and upper mantle structure in Japan, Part 1, Phase velocities of Love and Rayleigh waves in central Japan, *Bull. Earthq. Res. Inst.*, **44**, 489-494, 1966a.

Kaminuma, K., The crust and upper mantle structure in Japan, Part 3, An anisotropic model of the structure in Japan, *Bull. Earthq. Res. Inst.* **44**, 511-518, 1966b.

Kanamori, H., Study on the crust-mantle structure in Japan, Part 3, Analysis of surface wave data, *Bull. Earthq. Res. Inst.*, **41**, 811-818, 1963.

Kasahara, J., I. Suzuki, M. Kumazawa and K. Iida, Anisotropism of S waves in dunite, *J. Seism. Soc. Japan* (in Japanese), **21**, 229-236, 1968.

Kurita, T., Crustal and upper mantle structure in Japan from amplitude and phase spectra of long-period P waves, Part 1. Central mountain area, *J. Phys. Earth*, **17**, 13-41, 1969a; Part 2. Kanto Plain, *Spec. Contr. Geophys. Inst. Kyoto Univ.*, **9**, 137-166, 1969b; Part 3. Chugoku region, *J. Phys. Earth*, **18**, 53-78, 1970.

Kurita, T. and T. Mikumo, Inferences of a layered structure from S wave spectra, Part 1. Theoretical considerations on the S wave spectrum method, *J. Phys. Earth*, **19**, 93-110, 1971.

Kurita, T., Inferences of a layered structure from S wave spectra, Part 2. Crustal structure in selected regions of Japan, *J. Phys. Earth*, **19**, 111-142, 1971.

McEvilly, T. V., Central U. S. crust-mantle structure from Love and Rayleigh wave phase velocity inversion, *Bull. Seism. Soc. Am.*, **54**, 1997-2015, 1964.

Mikumo, T., A study on crustal structure in Japan by the use of seismic and gravity data, *Bull. Earthq. Res. Inst.*, **44**, 965-1007, 1966.

Phinney, R. A., Structure of the earth's crust from spectral behavior of long-period body waves, *J. Geophys. Res.*, **69**, 2997-3017, 1964.

Saito, M. and H. Takeuchi, Surface waves across the Pacific, *Bull. Seism. Soc. Am.*, **56**, 1067-1091, 1966.

Takeuchi, H., Y. Hamano and Y. Hasegawa, Rayleigh and Love wave discrepancy and the existence of magma pockets in the upper mantle, *J. Geophys. Res.*, **73**, 3349-3350, 1968.

Thatcher, W. and J. N. Brune, Higher mode interference and observed anomalous apparent Love wave phase velocities, *J. Geophys. Res.*, **74**, 6603-6611, 1969.

(Received June 9, 1971)